

# Identification of the internal ribosome entry sites in the 5'-untranslated region of the *c-fos* gene

HUI LI<sup>1\*</sup>, YUHANG CHEN<sup>1\*</sup>, JUNSHI ZHANG<sup>1</sup>, YONGQUAN LIN<sup>1</sup>,  
ZHILONG YANG<sup>2</sup>, JUAN TAN<sup>1</sup> and WENTAO QIAO<sup>1</sup>

<sup>1</sup>Key Laboratory of Molecular Microbiology and Technology, Ministry of Education, College of Life Sciences, Nankai University, Tianjin 300071, P.R. China; <sup>2</sup>Division of Biology, Kansas State University, Manhattan, KS 66506, USA

Received June 28, 2020; Accepted January 20, 2021

DOI: 10.3892/ijmm.2021.4889

**Abstract.** The Fos proto-oncogene, activator protein-1 (AP-1) transcription factor subunit (*c-fos*) gene, a member of the immediate early gene family, encodes c-Fos, which is a subunit of the AP-1 transcription factor. The present study aimed to investigate the mechanism by which the translation efficiency of *c-fos* mRNA is upregulated when cellular protein synthesis is shut off. The result of western blotting revealed that the protein expression levels of c-Fos were increased in rhabdomyosarcoma cells infected with enterovirus 71 (EV71) compared with uninfected cells. PCR was used to get the *c-fos* 5'-untranslated region (UTR). The luciferase assay of a bicistronic vector containing the *c-fos* 5'UTR revealed that the *c-fos* 5'UTR contains an internal ribosome entry site (IRES) sequence and a 175 nucleotide sequence (between 31 and 205 nt) that is essential for IRES activity. Analysis of potential IRES trans-acting factors revealed that poly(C)-binding protein 2 (PCBP2) negatively regulated the activity of the *c-fos* IRES, whereas the La autoantigen (La) positively regulated its activity. The results of RNA-protein immunoprecipitation demonstrated that both PCBP2 and La bound to the *c-fos* 5'UTR. Furthermore, the IRES activity of *in vitro*-transcribed *c-fos* mRNA was upregulated during EV71 infection. The present study suggested a mechanism for the effect of viral infection on host genes, and provided a novel target for gene translation regulation.

## Introduction

The Fos proto-oncogene, activator protein-1 (AP-1) transcription factor subunit (*c-fos*) gene is a proto-oncogene belonging to the immediate early gene family (1). c-Fos and c-Jun (a member of the Jun family of transcription factors) form a heterodimer through their leucine zipper plus basic domain (2), resulting in the formation of the AP-1 complex, which recognizes and binds AP-1 response elements in the promoter and enhancer regions of target genes, thus converting extracellular signals into changes in gene expression (3). c-Fos is involved in a number of important cellular events, including cell proliferation, differentiation and survival (4), and is activated by the MAPK-ERK1/2 signaling pathway, which also positively regulates enterovirus 71 (EV71) replication (5-8).

EV71 is a member of the *Picornaviridae* family, which are small non-enveloped, positive-strand RNA viruses with a genome size of ~7,400 nt. EV71 is the major etiological agent of hand, foot and mouth disease, which endangers global public health security (8). Additionally, this virus causes neurological disease and even death, particularly in young children (9,10). Picornavirus infection profoundly affects host cell mRNA translation (8). The 2A and 3C proteases of EV71 cleave eukaryotic translation initiation factor 4 (eIF4) G and poly(A) binding protein (PABP), respectively (11). The eIF4G protein is a component of the eIF4F cap-binding complex that is crucial for cap-dependent translation (11). PABP is an important factor for cellular mRNA translation that interacts with several translation initiation factors (11,12). Cleavage of eIF4G and PABP is considered to contribute to the shutdown of cellular protein synthesis (12).

Control of protein translation is crucial for cell proliferation, differentiation, mitosis and programmed apoptosis. Furthermore, abnormal regulation of translation initiation is often an important cause of tumors and disease (13-16). The translation initiation of most eukaryotic proteins relies on the mRNA 5'-m<sup>7</sup>G cap structure (12). However, certain RNA viruses, including EV71, can utilize internal ribosome entry site (IRES) sequences, which are located in mRNA 5'-untranslated regions (UTRs), to recruit the 40S ribosome directly to the vicinity of the initiation codon, independently of the cap structure (17,18).

Previous studies have demonstrated that numerous cellular genes also harbor IRES elements in the 5'UTR of their

---

**Correspondence to:** Dr Juan Tan or Dr Wentao Qiao, Key Laboratory of Molecular Microbiology and Technology, Ministry of Education, College of Life Sciences, Nankai University, 94 Weijin Road, Tianjin 300071, P.R. China  
E-mail: juantan@nankai.edu.cn  
E-mail: wentaoqiao@nankai.edu.cn

\*Contributed equally

**Key words:** internal ribosome entry site, internal ribosome entry site trans-acting factor, *c-fos*, enterovirus 71

mRNA (19,20). Cap-dependent initiation is compromised during mitosis, viral infection, hypoxia or apoptosis (19). A number of IRES-containing mRNAs use IRES-mediated translation to protect cells from stress conditions or to induce programmed cell death (19,21). Therefore, it was hypothesized that cellular IRES-mediated translation serves an important role in cellular processes under various conditions (22). For example, the IRES of the oncogene *c-myc* (23), the tumor suppressor gene *p53* (24) and the cellular transcription factor *c-jun* (25) can all contribute to the regulation of cellular activities. The latter pairs with c-Fos to form AP-1 (2).

The most obvious features of cellular IRES sequences are their GC-rich nature and length (>150 bases) (26). IRES sequences require IRES trans-acting factors (ITAFs) to recruit the 40S ribosomal subunit, and cellular IRES sequences promote the selective synthesis of certain proteins during situations when cap-dependent translation is compromised (27).

In our previous study, ribosome profiling revealed that the translation efficiency of *c-fos* was upregulated when cellular protein synthesis was stopped by EV71 infection, which may be regulated by IRES-mediated translation (28). The translation efficiency was defined as the relative increase in mRNA fragments protected by ribosomes (28). The present study investigated the mechanism by which the translation efficiency of *c-fos* mRNA is upregulated when cellular protein synthesis is shut off, and demonstrated the presence of an IRES element in the 5'UTR of the *c-fos* mRNA. Further analysis revealed that nucleotides 31-205 nt of the *c-fos* 5'UTR are essential for IRES-mediated translation. Furthermore, two well-known ITAFs, poly(C)-binding protein 2 (PCBP2) and La autoantigen (La), were found to regulate the activity of the *c-fos* IRES and to bind to the 5'UTR of the *c-fos* mRNA. In addition, EV71 infection activated the IRES in the *c-fos* 5'UTR and may contribute to the increase in c-Fos levels.

## Materials and methods

**Plasmid construction.** The bicistronic reporter vector pR-F and phpR-F constructs were gifts from Professor Anne E. Willis (MRC Toxicology Unit, University of Cambridge, Cambridge, UK) (29). The EV71 infectious clone, pSVA-EV71, was a gift from Professor Zhiyong Lou (Tsinghua University, Beijing, China). The empty Flag-tagged plasmid pCE-puro-3xFlag was a gift from Professor Akio Kihara (Faculty of Pharmaceutical Sciences, Hokkaido University, Sapporo, Japan) (30). Plasmid dl-mouse mammary tumour virus (MMTV) IRES, which contains the MMTV IRES sequence, was a gift from Professor Marcelo López-Lastra (Escuela de Medicina, Pontificia Universidad Católica de Chile, Santiago, Chile) (31). The aforementioned individuals are the original producers of the plasmids.

PCR was performed using DNA polymerase Ex Taq® (Takara Biotechnology Co., Ltd.) according to the manufacturer's protocol. The thermocycling conditions were as follows: 95°C for 5 min; 95°C for 30 sec, the annealing temperature was determined according to the primer T<sub>m</sub> value and reacted for 30 sec, the extension time was determined according to the length of the target fragment and the response was at 72°C; 95°C for 7 min; 4°C for preservation. A 2% agarose gel was used for electrophoresis, and ethidium bromide staining was

used to detect the target fragments. HeLa cells were used to create a cDNA library [for detailed methods, please refer to reverse transcription-quantitative (RT-qPCR) analysis] as the PCR template. The pSVA-EV71 plasmid was extracted by alkaline lysis method and used as the PCR template. The *gapdh* fragment and the coding regions of PTB, PCBP2, La, hnRNP K and P97 were PCR amplified from a cDNA library. The 5'UTR of *c-fos* was PCR amplified from cDNA library and the 5'UTR of EV71 was PCR amplified from pSVA-EV71. The full-length 5'UTR cDNA of the *c-fos* mRNA, the *gapdh* cDNA fragment (951-1,250 bp), the EV71 5'UTR and serial truncations of the *c-fos* 5'UTR were produced using PCR amplification with forward and reverse primers containing *EcoRI* and *NcoI* endonuclease restriction sites, respectively. All products were inserted separately into the dual luciferase vector pR-F between the *EcoRI* and *NcoI* sites, and the *c-fos* 5'UTR was also inserted into phpR-F between the *EcoRI* and *NcoI* sites. The *c-fos* 5'UTR was inserted upstream of the translation start codon of the firefly luciferase gene in the promoter-less pGL3-basic vector between the *MluI* and *BglII* sites. pGL3-basic, pGL3-SV40 and  $\beta$ -galactosidase ( $\beta$ -gal) were purchased from Promega Corporation. The coding regions of polypyrimidine tract-binding protein (PTB), PCBP2 and La were produced by PCR amplification using forward and reverse primers containing *BamHI* and *NotI* endonuclease restriction sites, while primers for the heterogeneous nuclear ribonucleoprotein (hnRNP) K and death-associated protein 5 (P97) coding regions contained *SalI* and *NotI* sites. These coding regions were separately inserted into the empty Flag-tagged plasmid pCE-puro-3xFlag between the *EcoRI* and *NcoI* sites or the *SalI* and *NotI* sites, respectively. All plasmids were verified using DNA sequencing (Sanger sequencing; performed by Sangon Biotech Co., Ltd.). The sequences of all forward and reverse primers were as follows: *c-fos* 5'UTR forward, 5'-GCGGAATTCATTCATAAAACGCTTGTTATAAAAGCAGTGGCTGCGG-3' and reverse, 5'-AATTATCCATGGCGTGGCGGTTAGGCAAAGCCGGG-3'; *gapdh* forward, 5'-CCGGAATTCATGATGACATCAAGAAGGTGGTGAAGC-3' and reverse, 5'-TATCCATGGTGAGGGTCTCTCTCTCTCTCTTG-3'; EV71 5'UTR forward, 5'-CAAGAATTCATAAAACAGCCTGTGGGTTGCACCCACTC-3' and reverse, 5'-GCCCCATGGTGTGTTGACTGTATTGAGAGTTAATATAAAGTTGAGGGGTG-3'; *c-fos* 5'UTR 1-30 forward, 5'-AATTCATTCATAAAACGCTTGTTATAAAAGCAGTGC-3' and reverse, 5'-CATGGCACTGCTTTTATAACAAGCGTTTTATGAATG-3'; *c-fos* 5'UTR 31-113 forward, 5'-ATAGAATTCGCTGCGGCGCCCTCGTACTCCAAC-3' (also used as the forward for *c-fos* 5'UTR 31-137, *c-fos* 5'UTR 31-164 and *c-fos* 5'UTR 31-185) and reverse, 5'-TATCCATGGTTCGCTGCGCCGCGCCGCTCAGTCTTG-3'; *c-fos* 5'UTR 114-205 forward, 5'-ATAGAATTCGAGCAGTGACCGTGCCTACCCAGC-3' and reverse, 5'-ATACCATGGCGTGGCGGTTAGGCAAAGCCGGG-3' (also used as the reverse for *c-fos* 5'UTR 45-205, *c-fos* 5'UTR 60-205, *c-fos* 5'UTR 75-205 and *c-fos* 5'UTR 93-205); *c-fos* 5'UTR 31-137 reverse, 5'-AATACCATGGTGGGTAGGAGCACGGCCACTG-3'; *c-fos* 5'UTR 31-164 reverse, 5'-TATCCATGGAGACAGGTGGGCGCTGTGAAG-3'; *c-fos* 5'UTR 31-185 reverse, 5'-TTATACCATGGGGGCGAGGGGCCGAGGGGCGGAGAC-3'; *c-fos* 5'UTR 45-205 forward, 5'-GTCGAATTCCTAC

TCCAACCGCATCTGCAGCGAGCAAC-3'; *c-fos* 5'UTR 60-205 forward, 5'-ATCGAATTCTGCAGCGAGCAACTGAGAAGCCAAGAC-3'; *c-fos* 5'UTR 75-205 forward, 5'-TATGAATTCAGAAAGCAAGACTGAGCCGGCGGCCGCGGCAGCGAAC-3'; *c-fos* 5'UTR 93-205 forward, 5'-ATTAGATTCTGGCGGCCGCGGCAGCGAACGAGCAG-3'; PTB forward, 5'-TATGGATCCATGGACGGCATTGTCCCAGATATAGCC-3' and reverse, 5'-TAATGCGGCCGCCTAGATGGTGGACTTGGAGAAGGAGAC-3'; PCBP2 forward, 5'-GAGGGATCCATGGACACCGGTGTGATTGAAGG-3' and reverse, 5'-ATTAGCGGCCGCCTAGCTGCTCCCATGCCACCCGTCTC-3'; La forward, 5'-GCGGGATCCATGGCTGAAAATGGTGATAATGAAAAGATGGC-3' and reverse, 5'-ATTAGCGGCCGCCTACTGGTCTCCAGCACCATTTTCTGTTTTCTG-3'; hnRNP K forward, 5'-TCAAGTCGACATGGAACTGAACAGCCAG-3' and reverse, 5'-GCATGCGGCCGCTTAGAAAACTTTCCAGAAT-3'; and P97 forward, 5'-AATAGTCGACATGGCTTCTGGAGCGATTC-3' and reverse, 5'-TATTGCGGCCGCTTAGCCATACAGGTCATCAT-3'.

**Cell culture and DNA transfection.** Human rhabdomyosarcoma (RD), HeLa and 293T cell lines (The Cell Bank of Type Culture Collection of The Chinese Academy of Sciences) were cultured in DMEM (Gibco; Thermo Fisher Scientific, Inc.) with 10% (v/v) FBS (HyClone; Cytiva), penicillin (100 U/ml) and streptomycin (100 µg/ml). All cells were cultured at 37°C in a humidified atmosphere with 5% CO<sub>2</sub>.

For transient DNA transfection, cells (1.2x10<sup>5</sup> cells/well) were seeded into 12-well plates at 24 h before transfection. DNA was transfected into cells using Lipofectamine<sup>®</sup> 2000 (Invitrogen; Thermo Fisher Scientific, Inc.) according to the manufacturer's protocol. Opti-MEM (Invitrogen; Thermo Fisher Scientific, Inc.) mixed with Lipofectamine<sup>®</sup> 2000 was used for the transfection of plasmids at room temperature for 20 min. Cell medium was replaced with complete culture medium at 6 h post-transfection, and after 48 h, the cells were rinsed twice with PBS, and cell extracts were prepared using 5X Passive Lysis Buffer (Promega Corporation).

The transfection amounts of plasmids were as follows: 200 ng for pR-F, pR-*gapdh*-F, pR-*c-fos* 5'UTR-F, pR-*EV71* 5'UTR-F, phpR-*c-fos* 5'UTR-F, pGL3-basic, pGL3-*c-fos* 5'UTR, pGL3-SV40, pR-*c-fos* 5'UTR-F truncations, and dl-MMTV IRES; 50 ng for β-gal; and 250 or 500 ng for pCE-puro-3xFlag, pCE-puro-3xFlag-PTB, pCE-puro-3xFlag-PCBP2, pCE-puro-3xFlag-La, pCE-puro-3xFlag-hnRNP K and pCE-puro-3xFlag-P97. Among them, pR-F, pR-*gapdh*-F, pGL3-basic and pCE-puro-3xFlag were used as negative controls.

**In vitro transcription.** A MEGAscript T7 High Yield Transcription Kit (Thermo Fisher Scientific, Inc.) was used to perform *in vitro* transcription. The templates were first linearized using *Bam*HI and then reacted according to the manufacturer's protocol. According to the supplier's instructions, ~80% of the product RNA had an m<sup>7</sup>G cap (New England BioLabs, Inc.) at the 5'end. An RNeasy Mini Kit (Qiagen GmbH) was used to purify the RNA. RNA quantified by UV spectrophotometry was transfected into HeLa or RD cells using Lipofectamine<sup>®</sup> 3000 (Invitrogen; Thermo Fisher

Scientific, Inc.) as aforementioned. Opti-MEM mixed with Lipofectamine<sup>®</sup> 3000 was used for the transfection of 200 ng RNA at room temperature for 20 min. The following plasmids were used for transcription *in vitro*: pR-F, pR-*gapdh*-F, pR-*c-fos* 5'UTR-F and pR-*EV71* 5'UTR-F.

**EV71 infection.** pSVA-EV71 was linearized using *Sal*I, transcribed into RNA *in vitro*, and then transfected into RD cells using Lipofectamine<sup>®</sup> 3000 as mentioned in the *in vitro* transcription subsection. After cell death, the culture supernatant was harvested and centrifuged at 13,000 x g for 1 min at room temperature to obtain EV71 particles. EV71 was expanded in RD cells for three generations. The titers of viruses were measured using a 50% tissue culture infective dose assay. Transfected or untransfected cells were infected with EV71 at an MOI of 5 with maintenance medium containing 2% (v/v) FBS.

**Luciferase assay.** *Renilla* luciferase (RL) and firefly luciferase (FL) dual-luciferase activities were measured using a Dual-Luciferase Reporter Assay System (Promega Corporation) and FL single-luciferase activity was measured using a Luciferase Assay System (Promega Corporation) according to the manufacturer's protocol, with the exception that only 100 µl of each reagent was used. For the pR-F series, FL activity was normalized to *Renilla* activity. For the pGL3 series, FL activity was normalized to β-gal activity. Signals were measured using a luminometer.

The plasmids used to measure dual luciferase activity were as follows: pR-F, pR-*gapdh*-F, pR-*c-fos* 5'UTR-F, pR-*EV71* 5'UTR-F, phpR-*c-fos* 5'UTR-F, dl-MMTV IRES and pR-*c-fos* 5'UTR-F truncations. The plasmids for transcription *in vitro* used to measure dual luciferase activity were as follows: pR-F, pR-*gapdh*-F, pR-*c-fos* 5'UTR-F and pR-*EV71* 5'UTR-F. The plasmids used to measure FL single-luciferase activity were as follows: pGL3-basic, pGL3-*c-fos* 5'UTR, pGL3-SV40 and β-gal. Lipofectamine<sup>®</sup> 2000 or Lipofectamine<sup>®</sup> 3000 (Invitrogen; Thermo Fisher Scientific, Inc.) was used for transfection as mentioned in the *in vitro* transcription and cell culture and DNA transfection subsections. At 48 h after transfection, the cell extracts were prepared using 5X Passive Lysis Buffer (Promega Corporation). For infection experiments, *in vitro*-transcribed pR-F, pR-*gapdh*-F, pR-*c-fos* 5'UTR-F and pR-*EV71* 5'UTR-F mRNA was transfected into RD cells. After 1 h, RD cells were infected EV71 for 6, 8 and 10 h, and then harvested for FL and RL activity measurements.

**Protein analysis.** Cells were washed once with ice-cold 1X PBS and lysed in buffer containing 50 mM TRIS (pH 7.4), 150 mM NaCl, 2 mM EDTA, 3% glycerol, 1% NP-40 and protease inhibitor cocktail (complete, EDTA-free; Roche Diagnostics) for 30 min on ice. Following centrifugation at 13,000 x g for 10 min at 4°C, the supernatant was mixed with 5X SDS loading buffer containing 250 mM TRIS (pH 6.8), 10% SDS (w/v), 50% glycerol (v/v), 5% 2-mercaptoethanol (v/v) and 0.5% Bromophenol Blue (w/v), and boiled for 10 min at 100°C. The concentration of the protein samples was determined using the BCA protein quantification kit (Beijing Dingguo Changsheng Biotechnology Co., Ltd.), and the loading amount was 20 µg per lane. Samples were resolved

using 10% SDS-PAGE and transferred onto a PVDF membrane (GE Healthcare). Membranes were blocked with 5% non-fat milk (in 1X PBS) for 45 min at room temperature, and then probed with the primary antibodies for 90 min at room temperature. The primary antibodies against c-Fos (cat. no. YM3469; 1:1,000) and Flag-tag (cat. no. YM3025; 1:5,000) were purchased from ImmunoWay Biotechnology Company. The primary antibody against Tubulin (cat. no. ab44928; 1:10,000) and the secondary goat anti-mouse IgG H&L (HRP) antibody (cat. no. ab6789; 1:10,000) were purchased from Abcam. Following incubation with the secondary antibody for 45 min at room temperature, the membranes were treated with Immobilon Western Chemiluminescent HRP Substrate (EMD Millipore) and protein signals were detected using X-ray film.

**RNA-protein immunoprecipitation (RIP).** Cells were co-transfected with 1  $\mu$ g pR-*c-fos* 5'UTR-F and 6  $\mu$ g of various ITAFs, as mentioned in the Cell culture and DNA transfection subsection. Lysates (900  $\mu$ l per IP reaction) were centrifuged at 1,000 x g at 4°C for 15 min and supernatants were aliquoted corresponding to 3x10<sup>6</sup> cells. A 6-mg anti-Flag antibodies (cat. no. YM3025; ImmunoWay Biotechnology Company) was crosslinked with 40  $\mu$ l magnetic Protein G Dynabeads (EMD Millipore). The crosslinked beads were incubated with aliquots of pre-cleared cell lysates at 4°C. After washing, immunoprecipitated RNA-protein complexes were eluted at 95°C. Eluates were treated for 10 min at room temperature with proteinase K (Beijing Dingguo Changsheng Biotechnology Co., Ltd.) and RNA was extracted using an RNeasy Mini Kit (Qiagen GmbH) and treated with DNaseI (Takara Biotechnology Co., Ltd.). cDNA synthesis and subsequent RT-PCR were performed as described subsequently. Western blotting was performed as aforementioned to detect protein expression. The buffer for cell lysis and immunoprecipitation consisted of 30 mM HEPES pH 7.3, 160 mM KCl, 2.5 mM MgCl<sub>2</sub>, 1 mM dithiothreitol (DTT), 0.1% NP-40, 0.5% Triton X-100 and 10% glycerol. The washing buffer contained PBS pH 7.4 and 0.02% Tween, and the elution buffer contained 100 mM TRIS-HCl pH 7.4, 5% SDS, 70 mM  $\beta$ -mercaptoethanol and 5 mM DTT.

**RT-qPCR analysis.** RD cells were lysed using TRIzol<sup>®</sup> reagent (Invitrogen; Thermo Fisher Scientific, Inc.). Total RNA was extracted using an RNeasy Mini Kit (Qiagen GmbH). Reverse transcription was performed with the oligoT primer (Shanghai Sangon Biotech Co., Ltd.), dNTPs (Takara Biotechnology Co., Ltd.) and M-MLV Reverse Transcriptase with 5X buffer (Promega Corporation). cDNA was synthesized at 42°C for 60 min. Thereafter, qPCR was carried out using 2X SYBR Green Mix (Roche Diagnostics). The sequences of the primers used were as follows: GAPDH (reference gene) forward, 5'-AACAGCGACACCCACTCTC-3' and reverse, 5'-CATAACAGGAAATGAGCTTGACAA-3'; cFOS forward, 5'-GGGGCAAGGTGGAACAGTTAT-3' and reverse, 5'-CCGCTTGAGTGTATCAGTCA-3'. The following thermocycling conditions were used: Initial denaturation at 95°C for 5 min, denaturing at 95°C for 15 sec and annealing and extension together at 60°C for 60 sec for 35 cycles. All oligoT primers and RT-PCR primers were synthesized by Sangon Biotech Co., Ltd. The final data were analyzed using the 2<sup>- $\Delta\Delta$ C<sub>q</sub></sup> method (32).

**RNA structure analysis.** The secondary structure of the *c-fos* 5'UTR was predicted by version 7.1 of the Geneious software (<https://www.geneious.com/>).

**Statistical analysis.** All experimental data were analyzed using GraphPad Prism 5.0 (GraphPad Software, Inc.) and presented as the mean  $\pm$  standard error of the mean. Each independent experiment was repeated at least twice. One-way ANOVA with Dunnett's multiple comparison test was used to analyze the statistical differences. P<0.05 was considered to indicate a statistically significant difference.

## Results

***c-Fos* expression is upregulated in EV71-infected RD cells.** Previously, ribosome profiling technology was used to analyze host gene expression in EV71-infected RD cells and it was demonstrated that the mRNA and translation efficiency of c-Fos were upregulated (28). *c-fos* mRNA expression was assessed using RT-qPCR, and 3.65-fold upregulation was observed at 6.25 h post infection, while the expression levels of the negative control (N-Myc interactor) remained unchanged, as expected (28) (Fig. 1A). c-Fos protein expression was also measured, and a marked increase in c-Fos expression was observed in EV71-infected RD cells at 6.25 h compared with mock cells (Fig. 1B).

**Identification and verification of an IRES element in the 5'UTR of *c-fos* mRNA.** To examine whether the high expression levels of c-Fos were regulated by an IRES-mediated mechanism, the *c-fos* 5'UTR was inserted into a bicistronic vector (pR-F), which contained RL and FL in the first and second cistrons, respectively. RL and FL were on the same mRNA, so RL was suitable for system calibration. FL/RL is usually used to show IRES activity (33,34). Additionally, two negative controls were included, comprising an empty vector containing the multiple cloning site in the intercistronic region (pR-F) and a vector containing a segment from the coding region of human *gapdh* (pR-*gapdh*-F). A plasmid containing the EV71 virus IRES (pR-EV71 5'UTR-F) was used as a positive control (Fig. 2A). The constructs were transfected into HeLa cells, and the luciferase activity was measured. The results suggested that the *c-fos* 5'UTR contained a potent IRES element that could direct a marked increase in the expression of the downstream cistron (Fig. 2B). However, other non-IRES-dependent causes, such as activation of a splicing event, readthrough or cryptic promoter activity, had to be eliminated.

To rule out an aberrant splicing event and ribosome readthrough, a hairpin structure was introduced at the transcription start site of the bicistronic reporter (Fig. 2C). The values of FL and RL were displayed separately, compared with bicistronics without hairpin, the hairpin only inhibited the expression of the upstream RL cistron, and in the presence of *c-fos* 5'UTR fragments, the expression of FL did not decrease but increased (Fig. 2D). This result suggested that an aberrant splicing event or ribosome readthrough could be eliminated as possible mechanisms (35).

To rule out cryptic promoter activities exerting an effect on the *c-fos* 5'UTR (36), the *c-fos* 5'UTR was inserted into the

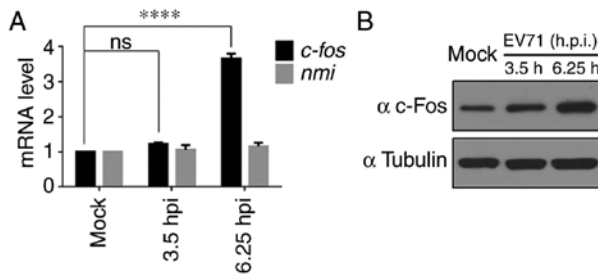


Figure 1. *c-Fos* expression is upregulated in RD cells infected with EV71. Infected RD cells were collected for (A) reverse transcription-quantitative PCR and (B) western blotting. The mock group was the uninfected control. Each experiment was independently repeated three times. \*\*\*\* $P < 0.0001$ . *c-fos*, Fos proto-oncogene, AP-1 transcription factor subunit; EV71, enterovirus 71; hpi, h post infection; *nmi*, N-Myc interactor; ns, not significant; RD, rhabdomyosarcoma.

pGL3-basic vector without a promoter (Fig. 2E). Compared with the pGL3-SV40 positive control, which contained an SV40-promoter, pGL3-*c-fos* did not exhibit significant promoter activity (Fig. 2F). Therefore, it was unlikely that the *c-fos* 5'UTR had cryptic promoter activity.

The activity of an IRES sequences may vary in different cell lines, and thus, it was examined whether the *c-fos* IRES activity would be different in 293T cells. Therefore, the pR-F series constructs were transfected into 293T cells. Compared with that in HeLa cells (Fig. 2B), the results revealed that the IRES activity of *c-fos* in 293T cells was reduced to 60% of that in HeLa cells; however, the IRES activity of EV71 in 293T cells was increased by 1.6-fold (Fig. 2G). This suggested that *c-fos* and EV71 had different IRES activities in different cell lines.

To confirm that *c-fos* IRES regulated translation but not transcription, and to exclude the effects of transcription and cryptic promoters, the pR-F series plasmids were transcribed *in vitro*, and the purified mRNA was subsequently transfected into HeLa cells. The cells were harvested at 8 h after transfection. Compared with the results of direct transfection of plasmids (Fig. 2B), the luciferase activity of the transfected mRNA was similar (Fig. 2H). This further demonstrated that there was an IRES element in the 5'UTR of the *c-fos* mRNA that regulated translation.

**Mapping the *c-fos* IRES element.** To further identify the core regions that promote the internal initiation of translation, serial truncations of the *c-fos* 5'UTR were created based on the secondary structure predicted by the Geneious software (Fig. 3A). Subsequently, different truncations were inserted into pR-F, and FL/RL was measured. The results revealed that the construct comprising nucleotides 31-205 maintained most of the IRES activity (Fig. 3B). Therefore, truncations of the 31-205 nt region from the 3'-terminus were created; however, it was observed that all truncations reduced the IRES activity (Fig. 3C). Subsequently, truncations of the *c-fos* 5'UTR 31-205 nt from the 5'-terminus were created, and as the fragments got shorter, the IRES activity gradually decreased (Fig. 3D). These results demonstrated that nucleotides 31-205 of the *c-fos* 5'UTR contributed to the maximal IRES activity, and further truncations would have a deleterious effect on the IRES activity.

**PCBP2 and La affect *c-fos* IRES activity by binding to the *c-fos* 5'UTR.** PTB, PCBP2, La, hnRNP K and P97 are well-characterized ITAFs that bind to the IRES region of mRNA and induce conformational changes to facilitate recruitment of the ribosome (31,37-40). Therefore, the present study aimed to evaluate the effect of overexpressing each of these five proteins on translation driven by the *c-fos* 5'UTR. Therefore, the pR-*c-fos* 5'UTR-F plasmid was co-transfected with different concentrations of plasmids expressing a Flag-tagged version of PTB, PCBP2, La, hnRNP K or P97 in 293T cells. PTB has been reported to be an ITAF of the MMTV IRES (31). Therefore, the dl-MMTV IRES and Flag-tagged PTB were co-transfected as a positive control. The results revealed that overexpression of PTB upregulated the IRES activity of MMTV (Fig. 4A), whereas PTB had little effect on *c-fos*-IRES activity (Fig. 4B). PCBP2 decreased *c-fos*-IRES activity (Fig. 4C), and the other three proteins enhanced *c-fos*-IRES activity (Fig. 4D-F). PCBP2, La and P97 were selected for further study to assess whether binding to the *c-fos* 5'UTR influenced the activity of the *c-fos* IRES.

Therefore, anti-Flag RIP was performed in 293T cells (Fig. 4G). Lysates were generated from 293T cells after co-transfection for 48 h. The hnRNP K [reported to interact with EV71 IRES (37)] and EV71 5'UTR were used as a positive control, and the 3xFlag vector served as a negative control. The results demonstrated that detectable products could be amplified from PCBP2 and La, but not P97, immunoprecipitated mRNA, indicating the physical interaction of PCBP2 and La with the *c-fos* 5'UTR. Overall, these results suggested that PCBP2 and La influenced the IRES activity of *c-fos* by binding to the *c-fos* 5'UTR.

***c-fos* 5'UTR-mediated translation is activated during EV71 infection of RD cells.** To investigate whether the upregulation of *c-Fos* in EV71-infected RD cells was caused by translation initiated by the *c-fos* 5'UTR, an infection confirmation experiment was performed. The pR-F series plasmids in Fig. 2A, which also contained a T7 promoter, were transcribed *in vitro* and an m<sup>7</sup>G cap was added. In the same mRNA, the expression of RL depended on the cap, while the expression of FL depended on the inserted fragments (Fig. 5A). The mRNA was transfected into RD cells, and cells were infected with 5 MOI of EV71 for 6, 8 and 10 h at 1 h after transfection. Finally, the luciferase activity was detected. The results demonstrated that the IRES activities of *c-fos* 5'UTR and EV71 were both significantly upregulated upon EV71 infection at 8 and 10 h (Fig. 5B). The IRES activity of the *c-fos* 5'UTR was activated during EV71 infection and the IRES of the *c-fos* 5'UTR, as a translational regulatory element on mRNA, at least partially contributed to the expression of *c-Fos* protein during infection. This provided an explanation for the mechanism by which EV71 infection upregulated *c-Fos* expression at the translation level.

A model was provided to summarize the present findings (Fig. 5C). After EV71 infects the host cell, the viral protease 2A cleaves eIF4G, shutting down cap-dependent translation of general host genes, resulting in stagnating of expression (12). At this time, the IRES activity of *c-fos* 5'UTR is activated by EV71 infection. The image of EV71 was taken from the study by Plevka *et al* (41).

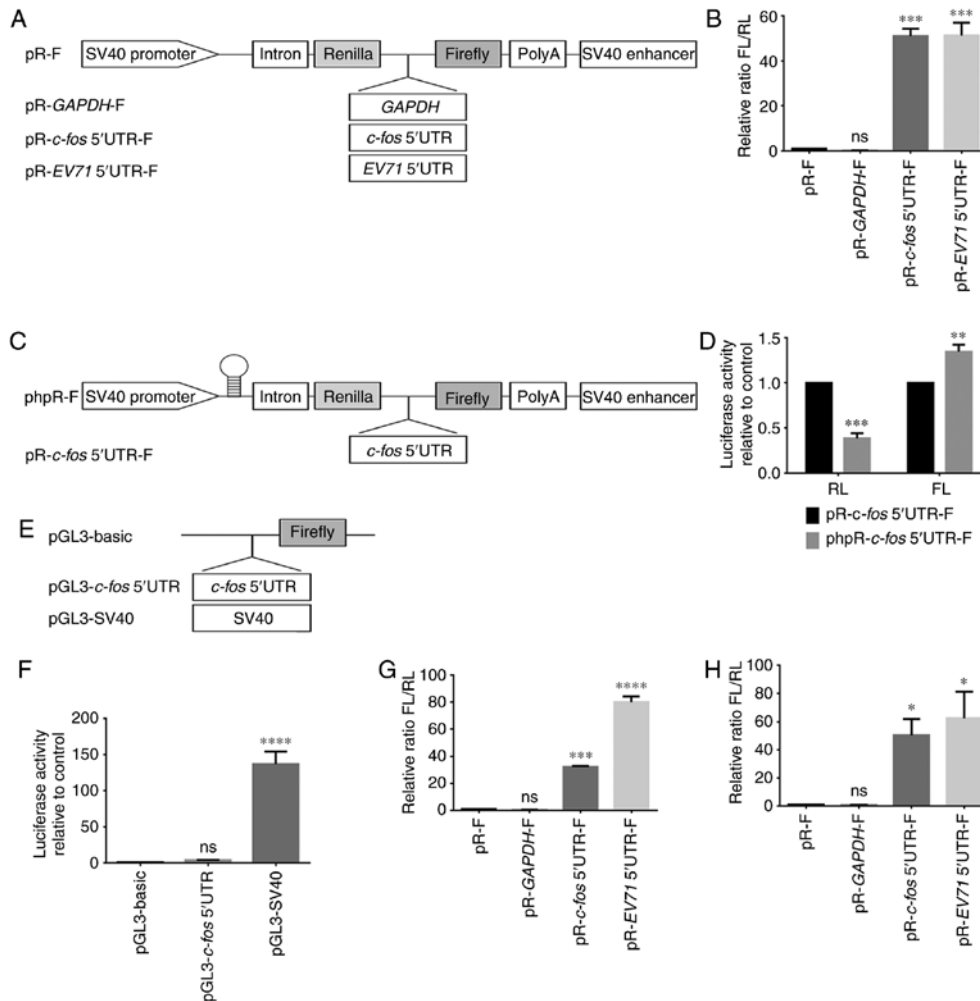


Figure 2. Identification of IRES activity in the *c-fos* 5'UTR. (A) Schematic representation of the expression cassette in the dual-luciferase bicronic constructs pR-F, pR-*gapdh*-F, pR-*c-fos* 5'UTR-F and pR-*EV71* 5'UTR-F. EV71 5'UTR was used as the positive control. (B) Plasmids pR-F, pR-*gapdh*-F, pR-*c-fos* 5'UTR-F and pR-*EV71* 5'UTR-F were transfected into HeLa cells. IRES activity was expressed as the ratio of downstream cistron expression to upstream cistron expression (FL/RL). pR-F was the control group. (C) Schematic representation of constructs phpR-F and phpR-*c-fos* 5'UTR-F, showing the introduction of a hairpin structure at the transcription start site of pR-F to rule out aberrant splicing events and ribosome readthrough. (D) pR-*c-fos* 5'UTR-F and phpR-*c-fos* 5'UTR-F were transfected into HeLa cells, and the RL and FL activities were measured. RL and FL of pR-*c-fos* 5'UTR-F were the control group. (E) To examine the cryptic promoter activity of the *c-fos* 5'UTR, the sequence was cloned into the promoterless pGL3-basic vector. The pGL3-SV40 was a positive control containing a promoter. (F) pGL3-basic, pGL3-*c-fos* 5'UTR and pGL3-SV40 were co-transfected with the  $\beta$ -gal plasmid into 293T cells. FL activity was measured and normalized against  $\beta$ -gal activity. pGL3-basic was the control group. (G) The same method as in (B) was performed in 293T cells. pR-F was the control group. (H) To exclude the influence of transcription levels and cryptic promoter, plasmids pR-F, pR-*gapdh*-F, pR-*c-fos* 5'UTR-F and pR-*EV71* 5'UTR-F were transcribed *in vitro*. The purified mRNA was transfected into HeLa cells to directly express luciferase. pR-F was the control group. Each experiment was independently repeated at least two times. \* $P < 0.05$ , \*\* $P < 0.01$ , \*\*\* $P < 0.001$  and \*\*\*\* $P < 0.0001$  vs. the respective control.  $\beta$ -gal,  $\beta$ -galactosidase; *c-fos*, Fos proto-oncogene, AP-1 transcription factor subunit; EV71, enterovirus 71; FL, firefly luciferase; IRES, internal ribosome entry site; ns, not significant; RL, *Renilla* luciferase; UTR, untranslated region; phpR-F, bicronic reporter vector containing hairpin; pR-F, bicronic reporter vector; pGL3, reporter vector without promoter; SV40, simian virus 40 promoter.

## Discussion

When cells are under stress, such as starvation, hypoxia or apoptosis, overall cellular cap-dependent translation tends to be turned off (19,22). However, under external stress, certain key mRNAs in cells initiate translation in an IRES-dependent manner (19,20). A variety of cellular genes have been reported to contain IRES elements, including *p53*, *c-myc* and *c-jun*, which forms a heterodimer with *c-fos* (24,25,42). A number of viruses can shut off the host cell gene expression system to gain a competitive advantage or for immune evasion (43-47). Therefore, studying the mechanisms by which certain genes are upregulated during infection will help understand the crucial proteins and signaling pathways that are active in host-virus

interactions. The present study identified an IRES element in the *c-fos* 5'UTR, determined its core region and identified two ITAFs of the IRES. Furthermore, it was observed that EV71 infection upregulated the IRES activity of *c-fos*. To the best of our knowledge, the present study was the first to report the identification of the IRES activity in the 5'UTR of the *c-fos* mRNA.

EV71 can induce host cap-dependent translation shutoff (48,49). The expression levels of numerous genes of the MAPK signaling pathway, including *c-fos*, are upregulated in EV71-infected RD cells (50). In our previous study, RNA-sequencing and ribosome profiling, two high-throughput techniques, were used to analyze gene expression in RD cells. When the general cap-dependent translation of host cell was

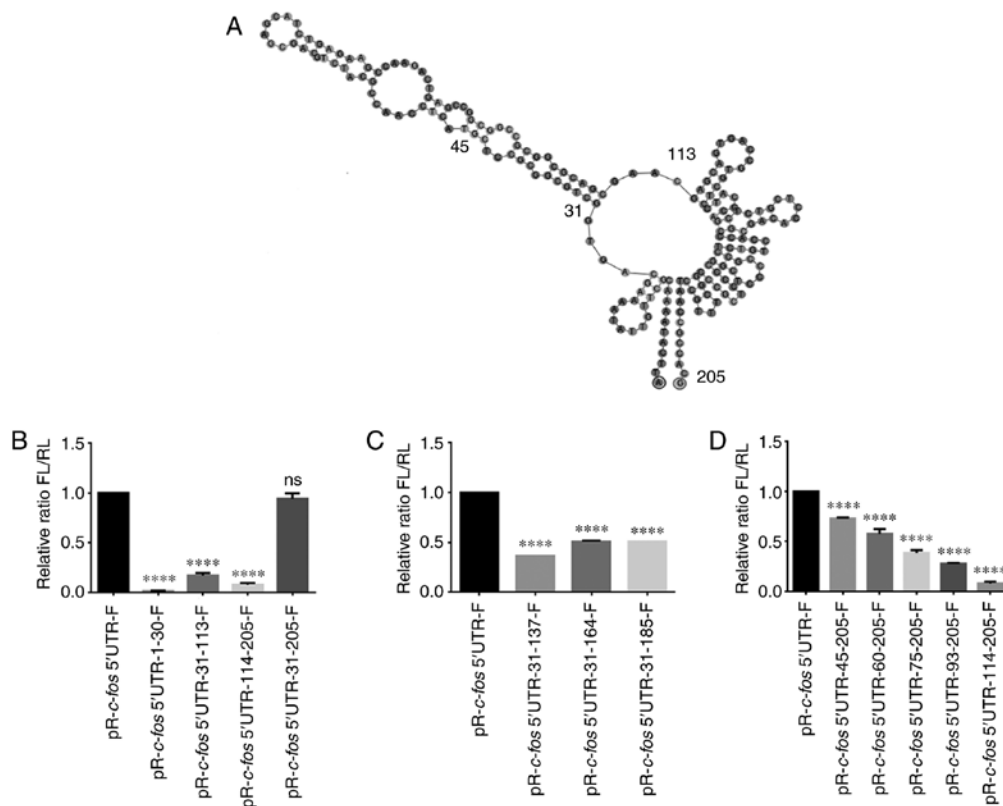


Figure 3. Mapping of the *c-fos* internal ribosome entry site. (A) Prediction of the secondary structure of the *c-fos* 5'UTR based on Geneious software analysis. (B) Bicistronic constructs containing a series of truncations of *c-fos* 5'UTR fragments were transfected into HeLa cells. (C) IRES activities of the truncations of the 31-205 nt region from the 3'-terminus. (D) IRES activities of the truncations of the 31-205 nt region from the 5'-terminus. Each experiment was independently repeated two times. \*\*\*\* $P < 0.0001$  vs. full-length *c-fos* 5'UTR. *c-fos*, Fos proto-oncogene, AP-1 transcription factor subunit; FL, firefly luciferase; IRES, internal ribosome entry site; ns, not significant; RL, *Renilla* luciferase; UTR, untranslated region; pR-F, bicistronic reporter vector.

turned off by EV71, *c-fos* translation efficiency was markedly upregulated (28). In the present study, the sequencing results were first verified and it was revealed that both the mRNA and protein levels of *c-fos* were increased during EV71 infection. Considering that the *c-fos* promoter was not markedly affected by EV71 (data not shown), it is possible that *c-fos* mRNA continues to be translated in a cap-independent manner, such as via an IRES.

In contrast to regular viral IRESs, cellular IRESs cannot be classified because they do not exhibit sequence or secondary structure similarities (20). Researchers have tried to use database analysis to predict cellular IRESs, such as analyses using IRSS, IRESfinder, IRESpy and IRESpred (51-54). However, the bicistronic test for IRES element verification remains the gold standard (51). The present study used the classic bicistronic reporter system to identify that the *c-fos* 5'UTR had strong IRES activity, comparable to that of the EV71 5'UTR, and ruled out non-IRES-mediated causes. Subsequently, two databases, IRESpy (53) and IRESpred (54), were used to make predictions. The results revealed that the *c-fos* 5'UTR had no typical IRES structures (data not shown). On the one hand, this further demonstrated that the true general characteristics of cellular IRESs have not yet been identified. On the other hand, it suggested that the *c-fos* IRES has a relatively special IRES structure, which is difficult to predict using the current IRES library. It was considered that the identification of the *c-fos* IRES adds novel information regarding the cellular IRES library.

The activity and function of an IRES is linked to its structure (55). Traditionally, 5'UTRs with high GC content may have IRES activity (26). The GC percentage of *c-fos* 5'UTR fragments was counted. The full-length *c-fos* 5'UTR GC content is 64%. The GC content of nucleotides 31-205, which retained the maximum IRES activity was 70%, corresponding to the middle large stem loop and a series of small hairpins at the 3'end. These analyses indicated that the GC-rich regions were favorable factors for the activity of the *c-fos* 5'UTR, and that the IRES activity was dependent on certain secondary structures, such as a complete stem-loop or hairpin combination. Further studies are required to determine the tertiary and 3D-folded structures of the *c-fos* 5'UTR. Thus, the present study provided a foundation for structural research in the future.

The majority of IRESs, particularly cellular IRESs, require ITAFs for their function (20). It has been reported that ~50 proteins have the ability to specifically regulate cellular IRESs (20). In the present study, PCBP2 downregulated and La upregulated the IRES activity of the *c-fos* 5'UTR dose-dependently and both of them interacted with *c-fos* 5'UTR mRNA. PCBP2 is involved in post-transcriptional and translational regulation by interacting with single-stranded poly(C) motifs in target mRNAs (38). Two adjacent CCCC sites in the *c-fos* 5'UTR that may interact with PCBP2 were observed. The La protein has been demonstrated to interact with a variety of cellular and viral RNAs and is involved in numerous cellular processes. Kumar *et al* (39) revealed that La interacts with the GCAC motif of the hepatitis C virus IRES

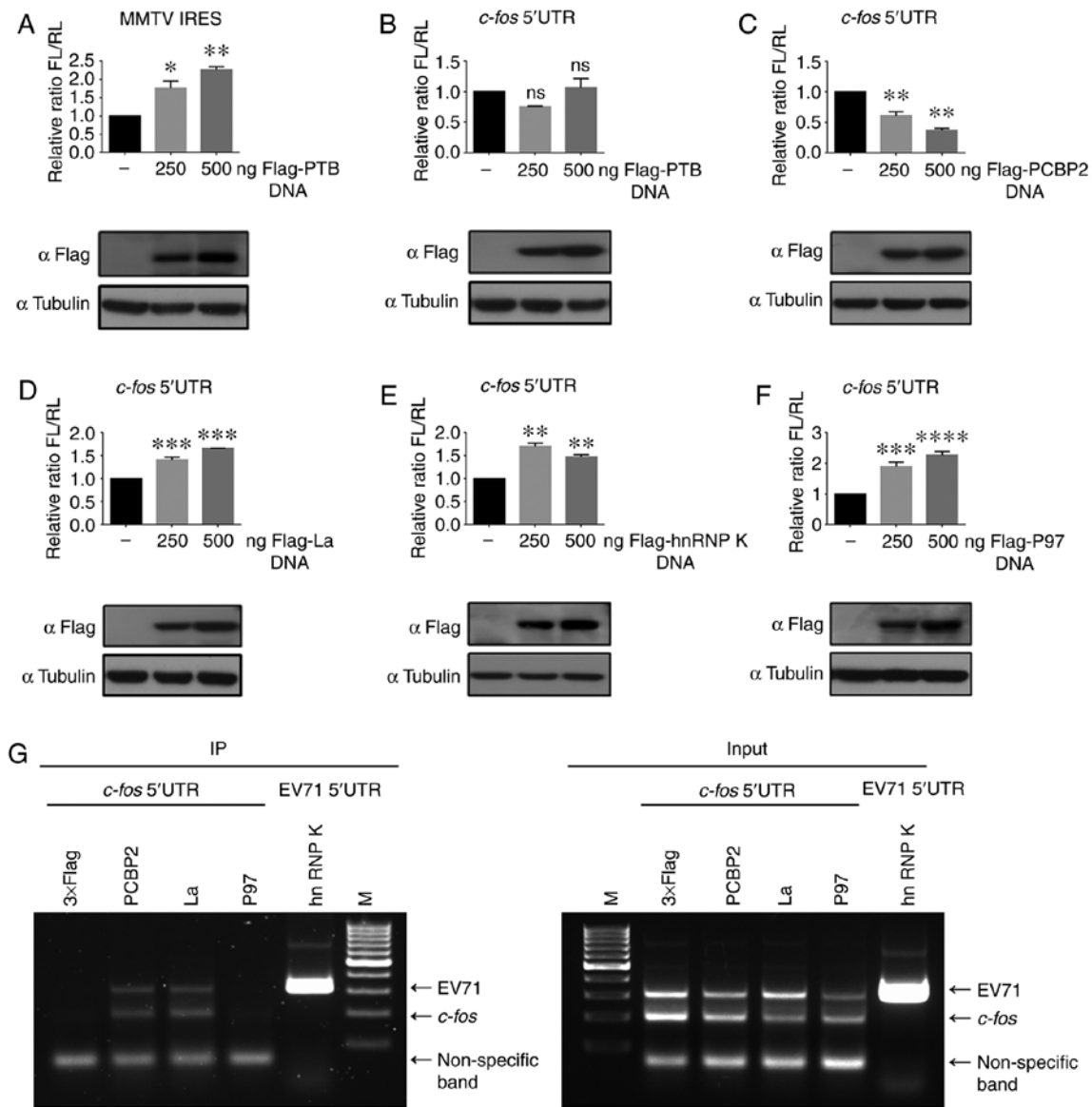


Figure 4. PCBP2 and La influence *c-fos* IRES activity by binding to the *c-fos* 5'UTR. (A) dl-MMTV IRES and 250 or 500 ng pCE-puro-3xFlag-PTB were co-transfected into 293T cells. Flag-PTB expression was detected by western blotting simultaneously. (B) Plasmid pR-*c-fos* 5'UTR-F and 250 or 500 ng pCE-puro-3xFlag-PTB were co-transfected into 293T cells, as in (A), to detect luciferase activity, followed by western blotting. (C) Plasmid pR-*c-fos* 5'UTR-F and 250 or 500 ng pCE-puro-3xFlag-PCBP2 were co-transfected. (D) Plasmid pR-*c-fos* 5'UTR-F and 250 or 500 ng pCE-puro-3xFlag-La were co-transfected. (E) Plasmid pR-*c-fos* 5'UTR-F and 250 or 500 ng pCE-puro-3xFlag-hnRNP K were co-transfected. (F) Plasmid pR-*c-fos* 5'UTR-F and 250 or 500 ng pCE-puro-3xFlag-P97 were co-transfected. (G) Identification of ITAFs interacting with the *c-fos* 5'UTR. There was a non-specific amplification band <100 bp at the bottom of the figure. Each experiment was independently repeated two times. \* $P < 0.05$ , \*\* $P < 0.01$ , \*\*\* $P < 0.001$  and \*\*\*\* $P < 0.0001$  vs. not transfected with ITAFs. *c-fos*, Fos proto-oncogene, AP-1 transcription factor subunit; EV71, enterovirus 71; FL, firefly luciferase; hnRNP K, heterogeneous nuclear ribonucleoprotein k; IRES, internal ribosome entry site; ITAFs, IRES trans-acting factors; La, La autoantigen; ns, not significant; P97, death-associated protein 5; PCBP2, poly(C)-binding protein 2; PTB, polypyrimidine tract-binding protein; RL, *Renilla* luciferase; UTR, untranslated region; dl-MMTV, bicistronic reporter vector containing MMTV IRES; IP, immunoprecipitation; M, marker; pR-F, bicistronic reporter vector.

to enhance viral RNA replication. There are six GCA sites in the *c-fos* 5'UTR representing candidate La interaction motifs. The specific interaction mechanisms require further experimental verification. It was attempted to knock down PCBP2 and La; however, no obvious impact on *c-fos* IRES activity was observed (data not shown), suggesting that there may be other functionally redundant ITAFs involved in *c-fos* IRES regulation. Overall, the present study identified PCBP2 and La as ITAFs for the *c-fos* IRES.

Picornavirus exerts complex regulatory effects of cellular IRESs (40,56). Polypyrimidine tract binding protein-associated splicing factor (PSF) protein levels are upregulated in

Coxsackievirus B3 (CVB3) infection, and the IRES element in the *psf* 5'UTR is activated during CVB3 infection (40). The EV71 3C protease cleaves the inhibitor protein hnRNP A1 of the apoptotic peptidase activating factor 1 (*apaf-1*) IRES, enabling IRES-dependent APAF-1 synthesis (56). The present study demonstrated experimentally that the IRES activity of pR-*c-fos* 5'UTR-F mRNA transcribed *in vitro* exhibited a trend of gradual upregulation during EV71 infection, providing a mechanism that explains how the virus upregulates *c-Fos* expression at the protein level. However, the molecular details of how EV71 activates the *c-fos* IRES, and the effects of *c-Fos* on EV71, require further exploration.

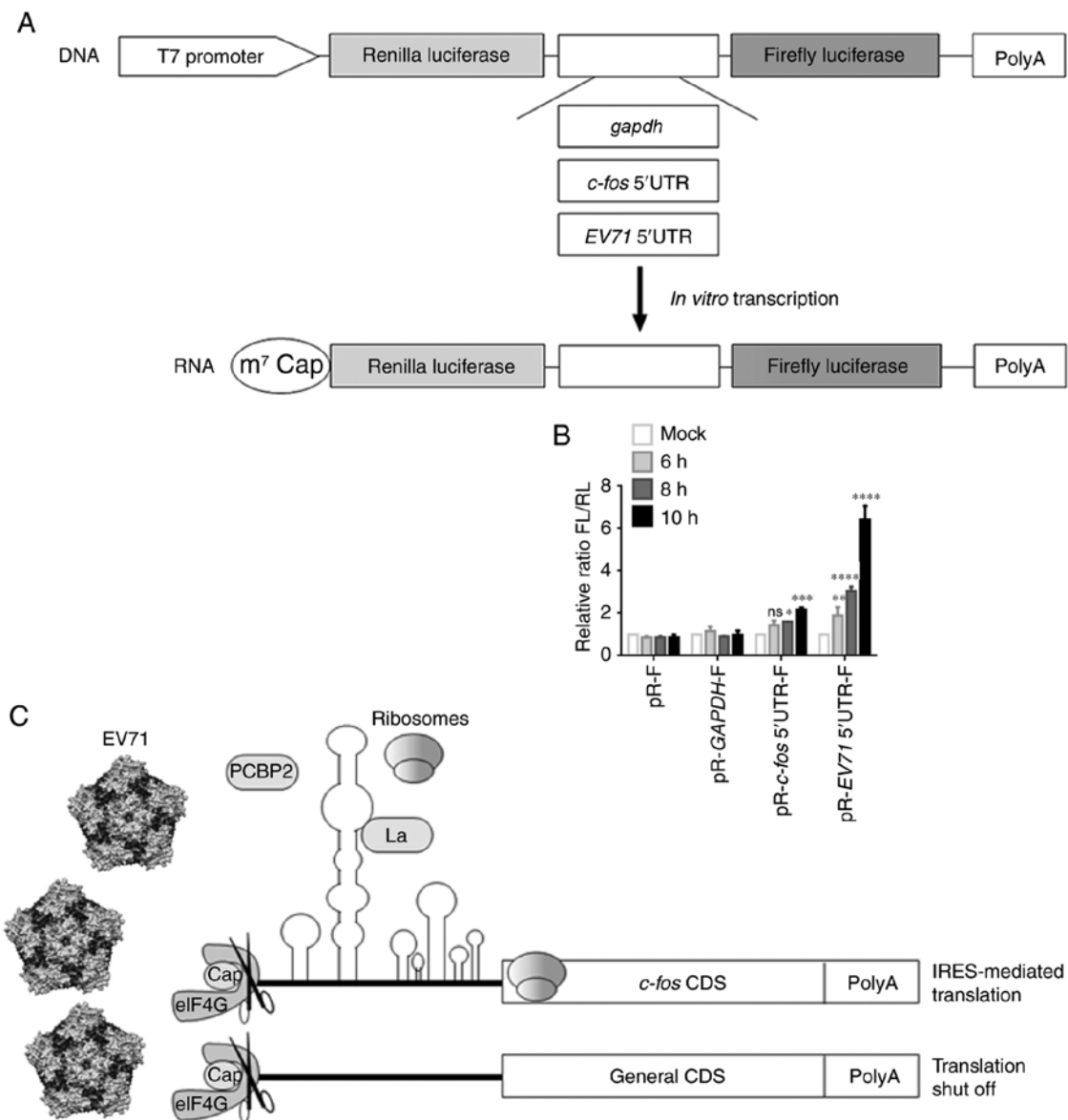


Figure 5. *c-fos* 5'UTR-mediated translation is activated in RD cells during EV71 infection. (A) Schematic diagram of the *in vitro* transcription construct. (B) *In vitro*-transcribed pR-F, pR-*gapdh*-F, pR-*c-fos* 5'UTR-F and pR-EV71 5'UTR-F mRNA was transfected into RD cells. After 1 h, RD cells were infected with EV71 for 6, 8 and 10 h, and then harvested for FL and RL activity measurements. EV71 5'UTR was used as the positive control. Each experiment was independently repeated two times. \*P<0.05, \*\*P<0.01, \*\*\*P<0.001 and \*\*\*\*P<0.0001 vs. mock. (C) Schematic diagram of the effect of EV71 infection on host gene mRNA translation. The image of EV71 was taken from the study by Plevka *et al* (41). *c-fos*, Fos proto-oncogene, AP-1 transcription factor subunit; eIF4G, eukaryotic translation initiation factor 4G; EV71, enterovirus 71; FL, firefly luciferase; IRES, internal ribosome entry site; La, La autoantigen; ns, not significant; PCBP2, poly(C)-binding protein 2; RD, rhabdomyosarcoma; RL, *Renilla* luciferase; UTR, untranslated region; cap, mRNA 5'-m7G cap structure; CDS, coding sequence; pR-F, bicistronic reporter vector.

In summary, previously, the regulation of c-Fos at the translational level was poorly understood; however, the present results demonstrated that EV71 upregulated *c-fos* IRES activity and c-Fos protein expression. The present results demonstrated the presence of IRES activity in the *c-fos* 5'UTR, which is likely to be a special cellular IRES structure. The present study provided a novel target that enriches the cellular IRES library.

#### Acknowledgements

The authors would like to thank Professor Anne E. Willis (MRC Toxicology Unit, University of Cambridge, Cambridge, UK), Professor Zhiyong Lou (Tsinghua University, Beijing,

China), Professor Marcelo López-Lastra (Escuela de Medicina, Pontificia Universidad Católica de Chile, Santiago, Chile) and Professor Akio Kihara (Faculty of Pharmaceutical Sciences, Hokkaido University, Sapporo, Japan) for providing plasmids.

#### Funding

The present study was supported by grants from the Key International Cooperation Project of National Key Research and Development Program of China (grant no. 2018YFE0107600; to WQ), the Natural Science Foundation of Tianjin (grant no. 19JCZDJC35700; to JT) and the National 973 Project of China (grant no. 2013CB911104; to JT).

## Availability of data and materials

The datasets used and/or analyzed during the current study are available from the corresponding author on reasonable request.

## Authors' contributions

HL, YC, JZ and YL performed experiments. HL and YC collated the data, drafted the manuscript and confirmed the authenticity of the data. ZY provided guidance on the design of experiments and made suggestions for the analysis of the results. JT supervised the experiments and provided general guidance and interpretation of the results. WQ designed the present study and provided feasible experimental proposals. All authors read and approved the final manuscript.

## Ethics approval and consent to participate

Not applicable.

## Patient consent for publication

Not applicable.

## Competing interests

The authors declare that they have no competing interests.

## References

- van Dam H and Castellazzi M: Distinct roles of Jun: Fos and Jun: ATF dimers in oncogenesis. *Oncogene* 20: 2453-2464, 2001.
- Shaulian E and Karin M: AP-1 as a regulator of cell life and death. *Nat Cell Biol* 4: E131-E136, 2002.
- Chiu R, Boyle WJ, Meek J, Smeal T, Hunter T and Karin M: The *c-fos* protein interacts with *c-Jun*AP-1 to stimulate transcription of AP-1 responsive genes. *Cell* 54: 541-552, 1988.
- Tulchinsky E: Fos family members: Regulation, structure and role in oncogenic transformation. *Histol Histopathol* 15: 921-928, 2000.
- Lim H and Kim HP: Matrix metalloproteinase-13 expression in IL-1 $\beta$ -treated chondrocytes by activation of the p38 MAPK/*c-Fos*/AP-1 and JAK/STAT pathways. *Arch Pharm Res* 34: 109-117, 2011.
- Hong S, Skaist AM, Wheelan SJ and Friedman AD: AP-1 protein induction during monopoiesis favors C/EBP: AP-1 heterodimers over C/EBP homodimerization and stimulates FosB transcription. *J Leukoc Biol* 90: 643-651, 2011.
- Duan H, Zhu M, Xiong Q, Wang Y, Xu C, Sun J, Wang C, Zhang H, Xu P and Peng Y: Regulation of enterovirus 2A protease-associated viral IRES activities by the cell's ERK signaling cascade: Implicating ERK as an efficiently antiviral target. *Antiviral Res* 143: 13-21, 2017.
- Shi W, Hou X, Peng H, Zhang L, Li Y, Gu Z, Jiang Q, Shi M, Ji Y and Jiang J: MEK/ERK signaling pathway is required for enterovirus 71 replication in immature dendritic cells. *Virology* 11: 227, 2014.
- Kehle J, Roth B, Metzger C, Pfitzner A and Enders G: Molecular characterization of an Enterovirus 71 causing neurological disease in Germany. *J Neurovirol* 9: 126-128, 2003.
- Schmidt NJ, Lennette EH and Ho HH: An apparently new enterovirus isolated from patients with disease of the central nervous system. *J Infect Dis* 129: 304-309, 1974.
- Chen LL, Kung YA, Weng KF, Lin JY, Horng JT and Shih SR: Enterovirus 71 infection cleaves a negative regulator for viral internal ribosomal entry site-driven translation. *J Virol* 87: 3828-3838, 2013.
- Thompson SR and Sarnow P: Enterovirus 71 contains a type I IRES element that functions when eukaryotic initiation factor eIF4G is cleaved. *Virology* 315: 259-266, 2003.
- Schmeing TM and Ramakrishnan V: What recent ribosome structures have revealed about the mechanism of translation. *Nature* 461: 1234-1242, 2009.
- Rodnina MV and Wintermeyer W: Recent mechanistic insights into eukaryotic ribosomes. *Curr Opin Cell Biol* 21: 435-443, 2009.
- Silvera D, Formenti SC and Schneider RJ: Translational control in cancer. *Nat Rev Cancer* 10: 254-266, 2010.
- Le Quesne JP, Spriggs KA, Bushell M and Willis AE: Dysregulation of protein synthesis and disease. *J Pathol* 220: 140-151, 2010.
- Hellen CU and Sarnow P: Internal ribosome entry sites in eukaryotic mRNA molecules. *Genes Dev* 15: 1593-1612, 2001.
- Balvay L, Soto Rifo R, Ricci EP, Decimo D and Ohlmann T: Structural and functional diversity of viral IRESes. *Biochim Biophys Acta* 1789: 542-557, 2009.
- Komar AA and Hatzoglou M: Internal ribosome entry sites in cellular mRNAs: Mystery of their existence. *J Biol Chem* 280: 23425-23428, 2005.
- Godet AC, David F, Hantelys F, Tatin F, Lacazette E, Garmy-Susini B and Prats AC: IRES trans-acting factors, key actors of the stress response. *Int J Mol Sci* 20: 2019.
- Sherrill KW, Byrd MP, Van Eden ME and Lloyd RE: BCL-2 translation is mediated via internal ribosome entry during cell stress. *J Biol Chem* 279: 29066-29074, 2004.
- Komar AA and Hatzoglou M: Cellular IRES-mediated translation: The war of ITAFs in pathophysiological states. *Cell Cycle* 10: 229-240, 2011.
- Stoneley M, Paulin FE, Le Quesne JP, Chappell SA and Willis AE: C-Myc 5' untranslated region contains an internal ribosome entry segment. *Oncogene* 16: 423-428, 1998.
- Yang DQ, Halaby MJ and Zhang Y: The identification of an internal ribosomal entry site in the 5'-untranslated region of p53 mRNA provides a novel mechanism for the regulation of its translation following DNA damage. *Oncogene* 25: 4613-4619, 2006.
- Blau L, Knirsh R, Ben-Dror I, Oren S, Kuphal S, Hau P, Proescholdt M, Bosserhoff AK and Vardimon L: Aberrant expression of *c-Jun* in glioblastoma by internal ribosome entry site (IRES)-mediated translational activation. *Proc Natl Acad Sci USA* 109: E2875-E2884, 2012.
- Sagliocco FA, Vega Laso MR, Zhu D, Tuite MF, McCarthy JE and Brown AJ: The influence of 5'-secondary structures upon ribosome binding to mRNA during translation in yeast. *J Biol Chem* 268: 26522-26530, 1994.
- Li Q, Gao WQ, Dai WY, Yu C, Zhu RY and Jin J: ATF2 translation is induced under chemotherapeutic drug-mediated cellular stress via an IRES-dependent mechanism in human hepatic cancer Bel7402 cells. *Oncol Lett* 12: 4795-4802, 2016.
- Lin Y, Wang Y, Li H, Chen Y, Qiao W, Xie Z, Tan J and Yang Z: Simultaneous and systematic analysis of cellular and viral gene expression during Enterovirus 71-induced host shutoff. *Protein Cell* 10: 72-77, 2019.
- Coldwell MJ, Mitchell SA, Stoneley M, MacFarlane M and Willis AE: Initiation of Apaf-1 translation by internal ribosome entry. *Oncogene* 19: 899-905, 2000.
- Ohno Y, Kihara A, Sano T and Igarashi Y: Intracellular localization and tissue-specific distribution of human and yeast DHHC cysteine-rich domain-containing proteins. *Biochim Biophys Acta* 1761: 474-483, 2006.
- Caceres CJ, Contreras N, Angulo J, Vera-Otarola J, Pino-Ajenjo C, Llorian M, Ameur M, Lisboa F, Pino K, Lowy F, *et al*: Polypyrimidine tract-binding protein binds to the 5' untranslated region of the mouse mammary tumor virus mRNA and stimulates cap-independent translation initiation. *FEBS J* 283: 1880-1901, 2016.
- Livak KJ and Schmittgen TD: Analysis of relative gene expression data using real-time quantitative PCR and the 2(-Delta Delta C(T)) method. *Methods* 25: 402-408, 2001.
- Gao G, Dhar S and Bedford MT: PRMT5 regulates IRES-dependent translation via methylation of hnRNP A1. *Nucleic Acids Res* 45: 4359-4369, 2017.
- Wein N, Vulin A, Falzarano MS, Szgyarto CA, Maiti B, Findlay A, Heller KN, Uhlén M, Bakthavachalu B, Messina S, *et al*: Translation from a DMD exon 5 IRES results in a functional dystrophin isoform that attenuates dystrophinopathy in humans and mice. *Nat Med* 20: 992-1000, 2014.
- Thompson SR: So you want to know if your message has an IRES? *Wiley Interdiscip Rev RNA* 3: 697-705, 2012.
- Kunze MM, Benz F, Brauss TF, Lampe S, Weigand JE, Braun J, Richter FM, Wittig I, Brüne B and Schmid T: sST2 translation is regulated by FGF2 via an hnRNP A1-mediated IRES-dependent mechanism. *Biochim Biophys Acta* 1859: 848-859, 2016.

37. Lin JY, Li ML, Huang PN, Chien KY, Horng JT and Shih SR: Heterogeneous nuclear ribonuclear protein K interacts with the enterovirus 71 5' untranslated region and participates in virus replication. *J Gen Virol* 89: 2540-2549, 2008.
38. Zhang X, Hua L, Yan D, Zhao F, Liu J, Zhou H, Liu J, Wu M, Zhang C, Chen Y, *et al*: Overexpression of PCBP2 contributes to poor prognosis and enhanced cell growth in human hepatocellular carcinoma. *Oncol Rep* 36: 3456-3464, 2016.
39. Kumar A, Ray U and Das S: Human La protein interaction with GCAC near the initiator AUG enhances hepatitis C Virus RNA replication by promoting linkage between 5' and 3' untranslated regions. *J Virol* 87: 6713-6726, 2013.
40. Dave P, George B, Sharma DK and Das S: Polypyrimidine tract-binding protein (PTB) and PTB-associated splicing factor in CVB3 infection: An ITAF for an ITAF. *Nucleic Acids Res* 45: 9068-9084, 2017.
41. Plevka P, Perera R, Cardoso J, Kuhn RJ and Rossmann MG: Crystal structure of human enterovirus 71. *Science* 336: 1274, 2012.
42. Le Quesne JP, Stoneley M, Fraser GA and Willis AE: Derivation of a structural model for the c-myc IRES. *J Mol Biol* 310: 111-126, 2001.
43. Fros JJ and Pijlman GP: Alphavirus Infection: Host cell shut-off and inhibition of antiviral responses. *Viruses* 8: 166, 2016.
44. Hoffmann M, Wu YJ, Gerber M, Berger-Rentsch M, Heimrich B, Schwemmle M and Zimmer G: Fusion-active glycoprotein G mediates the cytotoxicity of vesicular stomatitis virus M mutants lacking host shut-off activity. *J Gen Virol* 91: 2782-2793, 2010.
45. Vreede FT and Fodor E: The role of the influenza virus RNA polymerase in host shut-off. *Virulence* 1: 436-439, 2010.
46. Dremel SE and DeLuca NA: Herpes simplex viral nucleoprotein creates a competitive transcriptional environment facilitating robust viral transcription and host shut off. *Elife* 8: e51109, 2019.
47. Rutkowski AJ, Erhard F, L'Hernault A, Bonfert T, Schilhabel M, Crump C, Rosenstiel P, Efstathiou S, Zimmer R, Friedel CC and Dölken L: Widespread disruption of host transcription termination in HSV-1 infection. *Nat Commun* 6: 7126, 2015.
48. Bai J, Chen X, Liu Q, Zhou X and Long JE: Characteristics of enterovirus 71-induced cell death and genome scanning to identify viral genes involved in virus-induced cell apoptosis. *Virus Res* 265: 104-114, 2019.
49. Ho BC, Yu SL, Chen JJ, Chang SY, Yan BS, Hong QS, Singh S, Kao CL, Chen HY, Su KY, *et al*: Enterovirus-induced miR-141 contributes to shutoff of host protein translation by targeting the translation initiation factor eIF4E. *Cell Host Microbe* 9: 58-69, 2011.
50. Shi W, Hou X, Li X, Peng H, Shi M, Jiang Q, Liu X, Ji Y, Yao Y, He C and Lei X: Differential gene expressions of the MAPK signaling pathway in enterovirus 71-infected rhabdomyosarcoma cells. *Braz J Infect Dis* 17: 410-417, 2013.
51. Wu TY, Hsieh CC, Hong JJ, Chen CY and Tsai YS: IRSS: A web-based tool for automatic layout and analysis of IRES secondary structure prediction and searching system in silico. *BMC Bioinformatics* 10: 160, 2009.
52. Zhao J, Wu J, Xu T, Yang Q, He J and Song X: IRESfinder: Identifying RNA internal ribosome entry site in eukaryotic cell using framed k-mer features. *J Genet Genomics* 45: 403-406, 2018.
53. Wang J and Gribskov M: IRESpy: An XGBoost model for prediction of internal ribosome entry sites. *BMC Bioinformatics* 20: 409, 2019.
54. Kolekar P, Pataskar A, Kulkarni-Kale U, Pal J and Kulkarni A: IRESPred: Web server for prediction of cellular and viral internal ribosome entry site (IRES). *Sci Rep* 6: 27436, 2016.
55. Plank TD and Kieft JS: The structures of nonprotein-coding RNAs that drive internal ribosome entry site function. *Wiley Interdiscip Rev RNA* 3: 195-212, 2012.
56. Li ML, Lin JY, Chen BS, Weng KF, Shih SR, Calderon JD, Tolbert BS and Brewer G: EV71 3C protease induces apoptosis by cleavage of hnRNP A1 to promote apaf-1 translation. *PLoS One* 14: e0221048, 2019.